Trajectory Tracking of a Reconfigurable Multirotor Using Optimal Robust Sliding Mode Controller

Saddam Hocine Derrouaoui[1], Yasser Bouzid[1], Mohamed Guiatni[1] and Amina Belmouhoub[2]

Abstract— **This work aims to design a robust Sliding Mode Controller (SMC) in order to stabilize and follow the desired trajectory of a new reconfigurable multirotor. Due to changeable shape of the studied drone, the designed SMC in this work consists to ensure the robustness in the face of the parameters interaction, and various uncertainties of the system. In order to select the controller optimal parameters of each flight configuration, a Metaheuristic Algorithm based on Particle Swarm Optimization (PSO) is used. Nevertheless, the control architecture of this multirotor is different to the standard one, which makes it a very difficult task. To evaluate the effectiveness of the SMC, a simulation scenario is carried out, where the multirotor geometry is variable depending on the assigned tasks and environment.**

Index Terms— **Reconfigurable multirotor, Sliding Mode Controller (SMC), Optimization, PSO.**

I. Introduction

Currently, reconfigurable drones can adapt to different flight conditions, missions and environments, due to their adaptable and variable shapes, unlike the classic drones. They can negotiate narrow gaps, fly in cluttered environments, inspect sensitive locations and transport multiple objects without additional mechanisms [1] [2] [3].

Patnaik et *al.* [4] have proposed a special design of a reconfigurable UAV to support the collisions in flight, where a PID controller was exploited to stabilize it in attitude. The switching problem between the configurations in flight of a foldable UAV was treated in [5]. The obtained results have shown the efficacy of the used control scheme. The same drone has been proposed in [6], where an adaptive PID controller was used in order to stabilize this flying robot. In reference [7], the trajectory optimization of a reconfigurable Unmanned aerial–aquatic vehicle was investigated. To achieve this goal, a Teaching- and Learning-Based Optimization (TLBO) algorithm was exploited. In paper [8], a transformable aerial robot which can manipulate objects was modeled and controlled. Moreover, to avoid singular forms problem, the authors have added 1 degrees-of-freedom propeller in the drone structure. In work [9], a new design of a bio-ispired reconfigurable drone was analyzed. To actuate its arm-wing, cranks and gear mechanisms were used. In order to stabilize and control a reconfigurable drone in flight, a conventional PID was applied in [10]. In article [11], a new design of a Triphibious flying robot which can tilt its rotors was developed. This design is based on the classic quadrotor structure. However, the experiment tests of the motion control were not performed in this work. In reference [12], three algorithms (CS,PSO,CS-PSO) have been applied and tested on a mini UAV to optimize its PID controllers. The gains of the multirotor attitude fuzzy controller have been evaluated using PSO algorithm in [13].

This work is an extension of our previous works [14] [15] [16]. Unlike the strategies proposed in this new area, which are mainly based on linear controllers, in this manuscript, we will design a non linear SMC to ensure flight stability and evaluate its robustness against the parameters interaction, and various uncertainties of our special multirotor. The structure complexity, and the change of the configuration while flying make the control strategy a very challenging task, especially in the reconfiguration (transformation) step. The control loop in this work calculates instantly and considers all geometric changes differently from the control loops proposed in the literature sources. To choose the adequate SMC parameters of each flight configuration, the PSO algorithm is used.

II. Dynamic modeling

The CoG of the reconfigurable multirotor changes depending on the flight configuration. In addition, the system global inertia $\mathfrak{I}_{3\times3}(\alpha_i(t))$ changes also according to the multirotor configuration (see Figure 1).

The angular and the linear velocity vectors in the body frame, are given respectively as: $\varsigma = (p, q, r) \in \mathbb{R}^3$ and $\Lambda^m = (u, v, w)^T \in \mathbb{R}^3$.

$\Upsilon = (\varphi, \theta, \psi)^T \in \mathbb{R}^3$ represents the orientation of the multirotor and ξ=$(x, y, z)^T \in \mathbb{R}^3$ represents its position.

Using Newton-Euler principle, we can given the relation between the velocities and the external forces $f^m = (f^m_x, f^m_y, f^m_z)^T \in \mathbb{R}^3$ and moments $\tau^m = (\tau^m_x, \tau^m_y, \tau^m_z)^T \in \mathbb{R}^3$ as follows:

$$\begin{bmatrix} \mathfrak{m}\mathfrak{I}_{3\times3}(\alpha_i(t)) & O_{3\times3} \\ O_{3\times3} & \mathfrak{I}_{3\times3}(\alpha_i(t)) \end{bmatrix} \begin{bmatrix} \dot{\Lambda}^m \\ \dot{\varsigma} \end{bmatrix} + \begin{bmatrix} \varsigma \times \mathfrak{m}\Lambda^m \\ \varsigma \times \mathfrak{I}(\alpha_i(t))\varsigma \end{bmatrix} = \begin{bmatrix} f^m \\ \tau^m \end{bmatrix} \quad (1)$$

Remark: The development steps detail is found in our previous work [15].

[1]Saddam Hocine Derrouaoui, Yasser Bouzid and Mohamed Guiatni are with Complex Systems Control & Simulators Laboratory, Ecole Militaire Polytechnique, Algiers, Algeria. [2]Amina Belmouhoub is with Materials and Electronic Systems Laboratory, Université Mohamed El Bachir El Ibrahimi, Bordj Bou Arréridj, Algeria derrouaouish@gmail.com, yasseremp@gmail.com, mohamed.guiatni@gmail.com,belmouhoub.amina@gmail.com

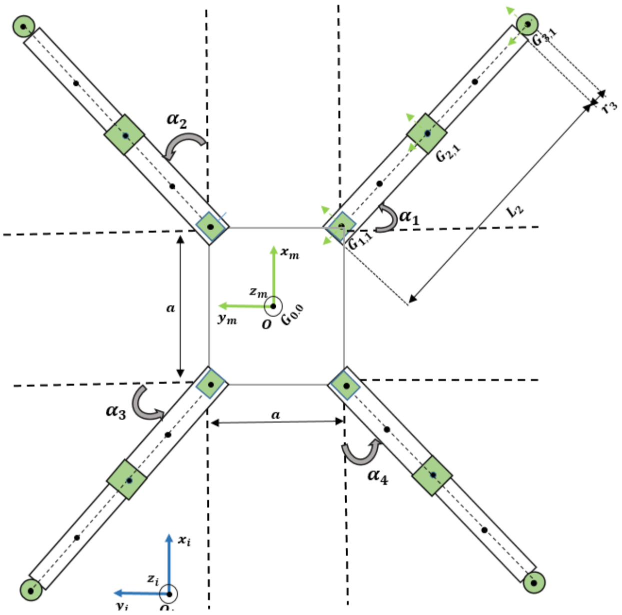

Fig. 1: Reconfigurable multirotor schematic.

III. Control

A. Multirotor control architecture

The SMC is designed to guarantee the tracking of the desired path and to be robust against different geometrical and inertial variations. The desired positions (x_d,y_d,z_d,ψ_d) are generated by a trajectory generator block as displayed in Figure 2. The configurations switch block, generates the desired α_{id}, and consequently the desired configuration depending on the assigned tasks and the flight environment. In addition, the rotation of the servomotors causes an important changes in the arm angles α_i. These angles are sent to the various blocks of the control loop to calculate instantly the CoG, inertia matrix and the control matrix.

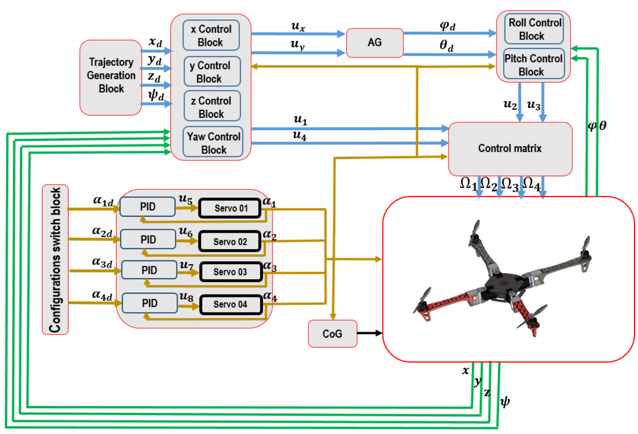

Fig. 2: Multirotor control architecture.

B. Sliding Mode Control (SMC) design

To design the SMC, we have used the control model as:

$$\begin{cases} \ddot{\varphi} &= \beta_1(t)\dot{\theta}\dot{\psi} + \beta_2(t)\dot{\theta}\Omega_r + \beta_3(t)u_2 + \beta_4(t)\dot{\varphi}^2 \\ \ddot{\theta} &= \beta_5(t)\dot{\varphi}\dot{\psi} + \beta_6(t)\dot{\varphi}\Omega_r + \beta_7(t)u_3 + \beta_8(t)\dot{\theta}^2 \\ \ddot{\psi} &= \beta_9(t)\dot{\theta}\dot{\varphi} + \beta_{10}(t)u_4 + \beta_{11}(t)\dot{\psi}^2 \\ \ddot{z} &= -g + u_1\frac{c_\varphi c_\theta}{m} + \beta_{12}\dot{z} \\ \ddot{x} &= u_1\frac{u_x}{m} + \beta_{13}\dot{x} \\ \ddot{y} &= u_1\frac{u_y}{m} + \beta_{14}\dot{y} \end{cases} \tag{2}$$

with

$\beta_1(t)=\frac{I_{yy}(\alpha_i(t)) - I_{zz}(\alpha_i(t))}{I_{xx}(\alpha_i(t))}$, $\beta_2(t)=\frac{-\mathfrak{J}_r}{I_{xx}(\alpha_i(t))}$

$\beta_3(t)=\frac{1}{I_{xx}(\alpha_i(t))}$, $\beta_4(t)=\frac{-\mathcal{K}_{\mathcal{A}x}}{I_{xx}(\alpha_i(t))}$

$\beta_5(t)=\frac{I_{zz}(\alpha_i(t)) - I_{xx}(\alpha_i(t))}{I_{yy}(\alpha_i(t))}$, $\beta_6(t)=\frac{\mathfrak{J}_r}{I_{yy}(\alpha_i(t))}$

$\beta_7(t)=\frac{1}{I_{yy}(\alpha_i(t))}$, $\beta_8(t)=\frac{-\mathcal{K}_{\mathcal{A}y}}{I_{yy}(\alpha_i(t))}$

$\beta_9(t)=\frac{I_{xx}(\alpha_i(t)) - I_{yy}(\alpha_i(t))}{I_{zz}(\alpha_i(t))}$, $\beta_{10}(t)=\frac{1}{I_{zz}(\alpha_i(t))}$

$\beta_{11}(t)=\frac{-\mathcal{K}_{\mathcal{A}z}}{I_{zz}(\alpha_i(t))}$, $\beta_{12}=\frac{-\mathcal{K}_{\mathcal{D}z}}{\mathfrak{m}}$, $\beta_{13}=\frac{-\mathcal{K}_{\mathcal{D}x}}{\mathfrak{m}}$, $\beta_{14}=\frac{-\mathcal{K}_{\mathcal{D}y}}{\mathfrak{m}}$

Usually, the SMC is composed of an attractive controller $\mathfrak{u}_a$ and an equivalent controller $\mathfrak{u}_e$ as:

$$\begin{aligned} u &= \mathfrak{u}_a + \mathfrak{u}_e \\ &= -\eta S - \sigma sign(S) + \mathfrak{u}_e \end{aligned} \tag{3}$$

where η, σ are positive parameters and S is the sliding surface.

The SMC corresponding to the first subsystem of (2), is obtained after some computations as:

$$\begin{aligned} u_2 = \frac{1}{-\beta_3(t)}&[\beta_1(t)\dot{\theta}\dot{\psi} + \beta_2(t)\dot{\theta}\Omega_r + \beta_4(t)\dot{\varphi}^2 - \ddot{\varphi}_d \\ &+ \mathfrak{N}_\varphi \dot{e}_1] - \eta_\varphi S_\varphi - \sigma_\varphi sign(S_\varphi) \end{aligned} \tag{4}$$

Theorem 1: *Using the designed controller (4), which corresponds to the first subsystem of (2), the asymptotic stability of the latter is guaranteed.*

Proof 1: *To prove **Theorem 1**, we choose firstly e_φ as a tracking error of the first subsystem (2):*

$$e_\varphi = \varphi - \varphi_d \tag{5}$$

The derivative of e_φ is given as:

$$\dot{e}_\varphi = \dot{\varphi} - \dot{\varphi}_d \tag{6}$$

Then, the sliding surface is constructed as:

$$S_\varphi = \dot{e}_\varphi + \mathfrak{N}_\varphi e_\varphi \tag{7}$$

where $\mathfrak{N}$ is a postive gain.
The derivative of the sliding surface S_φ is given as follows:

$$\dot{S}_\varphi = \ddot{e}_\varphi + \mathfrak{N}_\varphi \dot{e}_\varphi \tag{8}$$

By making $\dot{S}_\varphi = 0$, the equivalent controller $\mathfrak{u}_e$ is determined as the principal part of Equation (4).
Let us choose the Lyapunov function candidate as:

$$V_\varphi = \frac{1}{2}S_\varphi^2 \tag{9}$$

The derivative of V_φ is expressed as:

$$\dot{V}_\varphi = S_\varphi \dot{S}_\varphi \tag{10}$$

Replacing (4) and (8) in (10), we obtain:

$$\dot{V}_\varphi = -\eta_\varphi {S_\varphi}^2 - \sigma_\varphi |S_\varphi| < 0 \tag{11}$$

Clearly, the asymptotic stability is guaranteed by Equation 11

IV. Simulation and Interpretation

A. Simulation

The optimal controller's gains are given in Table I. These gains are found using the PSO algorithm and the objective function, which is based on Integral Square Error (ISE) as:

$$ISE = \int_{t_0}^{t_f} e_i^2(t)dt \tag{12}$$

where $i = 1, ..., 6$.

TABLE I: Optimal SMC parameters.

Parameter	Value
$\mathfrak{N}_\varphi$	5.31
$\mathfrak{N}_\theta$	5.78
$\mathfrak{N}_\psi$	4.61
$\mathfrak{N}_z$	4.89
η_φ	1.92
η_θ	0.8
η_ψ	1.41
η_z	1.23
σ_φ	2.15
σ_θ	3.25
σ_ψ	2.70
σ_z	1.19

Simulation results are given in the following Figures.

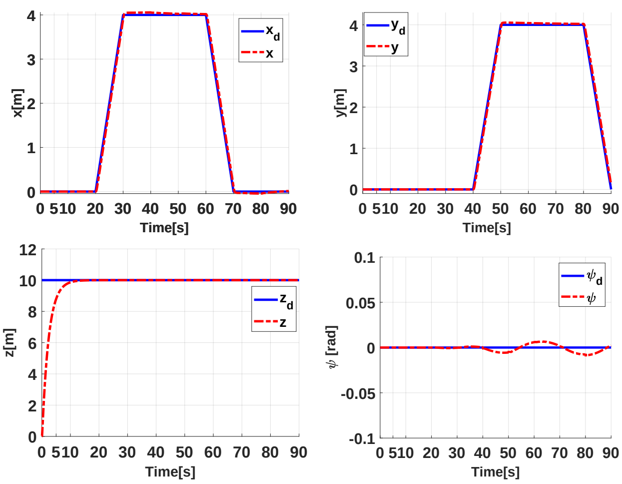

Fig. 3: Evolution of 3D trajectory and ψ angle.

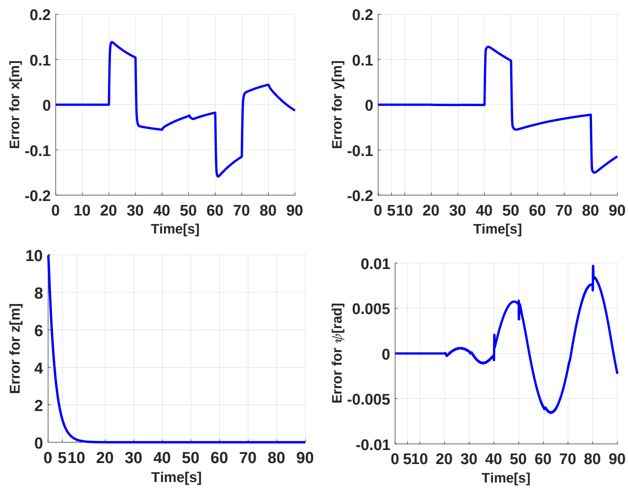

Fig. 4: Evolution of errors.

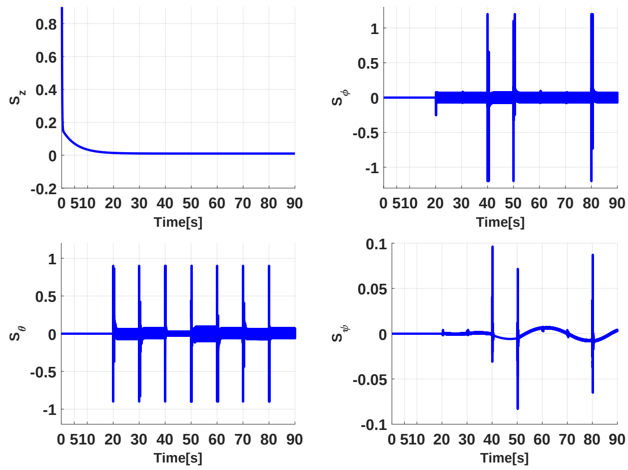

Fig. 5: Sliding surfaces.

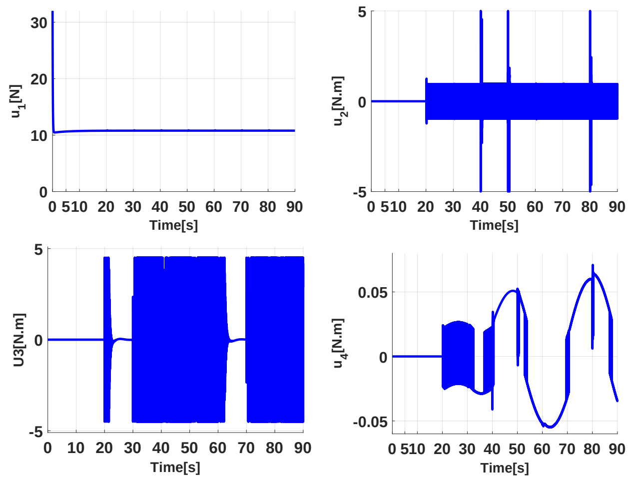

Fig. 6: Control signals.

B. Interpretation of the results

Figures 3 and 4 show clearly the performance of the SMC to track the desired path with a good accuracy and stability.

The controller u_1 displayed in Figure 6, which corresponds to the altitude z and the sliding surface S_z, it gets a maximum value in the start of the trajectory and then stabilizes around a constant value.

Figure 6 shows the evolution of the controllers u_2 and u_3. The variation of these signals is caused by the configuration changes of the multirotor.

The evolution of the yaw angle ψ is displayed in Figure 3, where we remark some weak oscillations in the outputs of the system. This is illustrated by the low value of the error in Figure 4 and the sliding surface S_ψ in Figure 5, and therefore the control signal u_4 in Figure 6.

From Figure 5, we can conclude that, the sliding surfaces converge rapidly towards zero.

Clearly, the chattering phenomena is appeared in the sliding surfaces and in the control signals (see Figures 5 and 6), and this is justified by the presence of the "$sign$" function. However, the SMC has ensured the convergence of the variable states to their desired states with high accuracy, and it has proven its robustness against the shape change of the multirotor in flight.

V. Conclusion

In this paper, we have introduced a novel multirotor that differs from a conventional one in the mechanical structure. This multirotor can unfold and fold its arms freely around the central body in different ways. Then, we have briefly presented the mathematical model, which represents the behavior of the proposed drone while flying. To ensure the stability in flight and reach the desired trajectory, a non linear SMC has been synthesized and applied. The robustness of the designed controller was tested through a simulation scenario in the face of the parameters interaction, and various uncertainties of the system. Simulation results have shown that, the SMC has proven its effectiveness in the control of this new type of drones.

References

[1] S. H. Derrouaoui, Y. Bouzid, M. Guiatni, and I. Dib, "A comprehensive review on reconfigurable drones: Classification, characteristics, design and control technologies," *Unmanned Systems*, pp. 1–27, 2021.

[2] S. H. Derrouaoui, Y. Bouzid, and M. Guiatni, "Pso based optimal gain scheduling backstepping flight controller design for a transformable quadrotor," *Journal of Intelligent & Robotic Systems*, vol. 102, no. 3, pp. 1–25, 2021.

[3] ——, "Towards a new design with generic modeling and adaptive control of a transformable quadrotor," *The Aeronautical Journal*, vol. 125, no. 1294, pp. 2169–2199, 2021.

[4] K. Patnaik, S. Mishra, Z. Chase, and W. Zhang, "Collision recovery control of a foldable quadrotor," *arXiv preprint arXiv:2105.12273*, 2021.

[5] A. Papadimitriou and G. Nikolakopoulos, "Switching model predictive control for online structural reformations of a foldable quadrotor," in *IECON 2020 The 46th Annual Conference of the IEEE Industrial Electronics Society*. IEEE, 2020, pp. 682–687.

[6] V. Riviere, A. Manecy, and S. Viollet, "Agile robotic fliers: A morphing-based approach," *soft robotics*, vol. 5, no. 5, pp. 541–553, 2018.

[7] X. Su, Y. Wu, F. Guo, J. Cui, and G. Yang, "Trajectory optimization of an unmanned aerial–aquatic rotorcraft navigating between air and water," *International Journal of Advanced Robotic Systems*, vol. 18, no. 2, p. 1729881421992258, 2021.

[8] M. Zhao, T. Anzai, K. Okada, K. Kawasaki, and M. Inaba, "Singularity-free aerial deformation by two-dimensional multilinked aerial robot with 1-dof vectorable propeller," *IEEE Robotics and Automation Letters*, vol. 6, no. 2, pp. 1367–1374, 2021.

[9] A. Lessieur, E. Sihite, P. Dangol, A. Singhal, and A. Ramezani, "Mechanical design and fabrication of a kinetic sculpture with application to bioinspired drone design," in *Unmanned Systems Technology XXIII*, vol. 11758. International Society for Optics and Photonics, 2021, p. 1175806.

[10] O. Köse and T. OKTAY, "Non simultaneous morphing system desing for quadrotors," *Avrupa Bilim ve Teknoloji Dergisi*, no. 16, pp. 577–588, 2019.

[11] G. Zhong, J. Cao, X. Chai, and Y. Bai, "Design and performance analysis of a triphibious robot with tilting-rotor structure," *IEEE Access*, vol. 9, pp. 10 871–10 879, 2021.

[12] N. El Gmili, M. Mjahed, A. El Kari, and H. Ayad, "Particle swarm optimization and cuckoo search-based approaches for quadrotor control and trajectory tracking," *Applied Sciences*, vol. 9, no. 8, p. 1719, 2019.

[13] J.-S. Chiou, H.-K. Tran, M.-Y. Shieh, and T.-N. Nguyen, "Particle swarm optimization algorithm reinforced fuzzy proportional–integral–derivative for a quadrotor attitude control," *Advances in Mechanical Engineering*, vol. 8, no. 9, p. 1687814016668705, 2016.

[14] Y. Bouzid, S. H. Derrouaoui, and M. Guiatni, "Pid gain scheduling for 3d trajectory tracking of a quadrotor with rotating and extendable arms," in *2021 International Conference on Recent Advances in Mathematics and Informatics (ICRAMI)*. IEEE, 2021, pp. 1–4.

[15] S. H. Derrouaoui, Y. Bouzid, M. Guiatni, I. Dib, and N. Moudjari, "Design and modeling of unconventional quadrotors," in *2020 28th Mediterranean Conference on Control and Automation (MED)*. IEEE, 2020, pp. 721–726.

[16] S. H. Derrouaoui, M. Guiatni, Y. Bouzid, I. Dib, and N. Moudjari, "Dynamic modeling of a transformable quadrotor," in *2020 International Conference on Unmanned Aircraft Systems (ICUAS)*. IEEE, 2020, pp. 1714–1719.